Thin Solid Films 636 (2017) 458–463

Contents lists available at ScienceDirect

Thin Solid Films

journal homepage: www.elsevier.com/locate/tsf

Structural and piezo-ferroelectric properties of $K_{0.5}Na_{0.5}NbO_3$ thin films grown by pulsed laser deposition and tested as sensors

R. Castañeda-Guzmán [a,*], R. López-Juárez [b], J.J. Gervacio [c], M.P. Cruz [c], S. Díaz de la Torre [d], S.J. Pérez-Ruiz [a]

[a] Centro de Ciencias Aplicadas y Desarrollo Tecnológico, Universidad Nacional Autónoma de México, Circuito Exterior S/N, Ciudad Universitaria, A.P. 70-186 C.P., 04510 México, DF, Mexico
[b] Unidad Morelia del Instituto de Investigaciones en Materiales, Universidad Nacional Autónoma de México, Antigua Carretera a Pátzcuaro No. 8701, Col. Ex Hacienda de San José de la Huerta, C.P. 58190 Morelia, Michoacán, Mexico
[c] Centro de Nanociencias y Nanotecnología, Universidad Nacional Autónoma de México, A. P. 356, C.P. 22800 Ensenada, BC, Mexico
[d] Instituto Politécnico Nacional, Centro de Investigación e Innovación Tecnológica CIITEC,, C.P. 02250, Azcapotzalco, México, DF, Mexico

ARTICLE INFO

Article history:
Received 7 October 2016
Received in revised form 26 May 2017
Accepted 18 June 2017
Available online 19 June 2017

Keywords:
Thin films
Ferroelectricity
Piezoelectricity
Piezoresponse force microscopy, photoacoustic

ABSTRACT

We have grown $K_{0.5}Na_{0.5}NbO_3$ (KNN) films on $Pt/TiO_2/SiO_2/Si$ substrates by using pulsed laser deposition. Thin films with pure KNN crystal phase and homogenous morphology were successfully prepared by optimizing the deposition conditions, mainly the oxygen partial pressure and deposition temperature. For oxygen pressure as low as 8 Pa a tungsten-bronze phase is formed, while for higher values i.e. 16 and 32 Pa, the desired KNN perovskite structure is obtained. To prepare pure KNN thin films, a deposition temperature as low as 675 °C is required, however, increasing the temperature to 725 °C promotes better homogeneity and densification of the films. The piezoelectric and ferroelectric behavior, confirmed by piezoresponse force microscopy, revealed a local piezoelectric coefficient of $d_{33} = 37$ pm/V and a coercive voltage of 3.5 V. Finally, we measured the frequency response of this material prepared as a sensor, using the photoacoustic method. This measurement shows that the resonant frequency of a KNN thin film of 230 nm thickness is centered at 3 MHz.

1. Introduction

Ferroelectric materials are widely used for many applications, such as actuators, sensors and buzzers [1]. Until now, the most used compound for these applications is $Pb(Ti,Zr)O_3$ (PZT), which contains around 60 Wt% of lead, which is a toxic element. Currently, many workers are developing the lead-free ferroelectrics needed to replace PZT. One of the most promising lead-free ceramics is $K_{0.5}Na_{0.5}NbO_3$ (KNN) [2–4], because of its high Curie temperature and remnant polarization [4–5]. KNN films have been prepared by different methods, including sol-gel, pulsed laser deposition (PLD) and sputtering [6–14]. By the Sol-gel method, high purity KNN films can be obtained, but it requires expensive and unstable reagents (niobium alkoxide) [6–7]. In addition, an excess of K^+ and Na^+ is needed to reduce departure from stoichiometry [8–9]. Thin films prepared by this technique show piezoelectric constants (d_{33}) ranging from 17 to 74 pm/V, depending on the excess of alkaline elements added [6–7]. On the other hand, sputtering and PLD are easier and demand inexpensive reagents [10–11,13]. Using sputtering, and different substrates, local d_{33} coefficients of 26 to 58 pm/V were measured [12] while, for PLD, values of 49 pm/V for Li^{+1}-Ta^{+5} co-doped KNN have been reported [10]. However, in all of these cases, ferroelectric hysteresis loops of films with thicknesses under 250 nm have not been found, perhaps due to the large number of defects, mostly caused by the K^+ and Na^+ losses. In this work, it is shown that by optimizing the deposition parameters in the PLD process, pure KNN films with less than 200 nm thicknesses can be prepared, with well-defined piezo-ferroelectric response determined by piezoresponse force microscopy. We show that these films can be used as sensors.

2. Experimental

The ceramic target used for film deposition was obtained by the solid state reaction of stoichiometric amounts of K_2CO_3, Na_2CO_3 and Nb_2O_5. The reagents, mixed using an agate mortar and acetone, were calcined at 850 °C for 1 h. Then, the powders were compacted into a pellet under 300 MPa using a uniaxial press. Once the pellet was sintered at 1060 °C for 2 h, it was used to grow thin films on $Pt/TiO_2/SiO_2/Si$ substrates. During film deposition, the fluence of the laser pulse and target to substrate distance were kept constant at 3 mJ/cm^2 and 5 cm, respectively. The substrate temperature was varied between 650 °C and 800 °C. The oxygen partial pressure was changed at 8, 16 and 32 Pa. The repetition rate was set at 5 or 10 Hz. Table 1 shows the growth conditions for the most representative samples. In order to confirm the target and film crystal structure, X-ray diffraction (XRD) patterns were collected in a Bruker D8 diffractometer, using Cu-Kα_1 (1.5406 Å) radiation.

* Corresponding author.
E-mail address: rosalba.castaneda@ccadet.unam.mx (R. Castañeda-Guzmán).

http://dx.doi.org/10.1016/j.tsf.2017.06.039
0040-6090/

Table 1
Growth conditions for KNN films.

Sample	Oxygen pressure (Pa)	Temp. (°C)
KNN1	8	700
KNN2	16	700
KNN3	16	675
KNN4	16	750
KNN5	16	800
KNN6	32	700
KNN7	32	725

For crystal size and morphology observations, a JEOL 7600F field emission scanning electron microscope (SEM) was employed. Piezoelectric properties, ferroelectric domains and local phase ferroelectric hysteresis loops were determined by piezoresponse force microscopy (PFM) and contact resonance (CR)-PFM, in a Dimension 3100 Nanoscope IV scanning probe microscope (SPM) System (Veeco). Platinum tips, 25Pt300B (Rocky Mountain Nanotechnology) and an *ac* bias of 10 Vpp were used.

3. Results and discussion

The synthesis of KNN ceramics has been demonstrated to be difficult due to potassium and sodium volatility at high temperature [4,15]. As a result, the presence of secondary phases, which strongly diminish the ferroelectric and piezoelectric properties, is common. Our ceramic target, however, does not show any secondary phases and only a pure perovskite KNN is obtained (Fig. 1).

The analysis of the films obtained is described below, starting with one representative sample i.e. the one grown at 16 Pa oxygen pressure, 800 °C and 10 Hz (marked as KNN5 in Table 1), followed by a description of the effects of changes in the deposition parameters. The KNN sample shows a pure orthorhombic KNN crystal phase, as can be seen in the top XRD pattern of Fig. 1, which agree with the data reported in literature [8,16–17]. The lattice parameters extracted from the XRD for the ceramic target are $a = 4.0192$, $b = 3.9628$ and $c = 4.0179$ Å, respectively. While for the KNN5 film are $a = 3.9767$ and $b = 3.9755$ Å, respectively. Furthermore, (100) preferential orientation is observed, this is due to the influence of the substrate, mainly the influence of Pt that also induces a slightly change in *a* lattice parameter, as reported before [17–18] and clearly evidenced in the values mentioned before. The morphology is composed of a loosely packed quasi-columnar growth over a denser and homogenous layer as can be appreciated in Fig. 2.

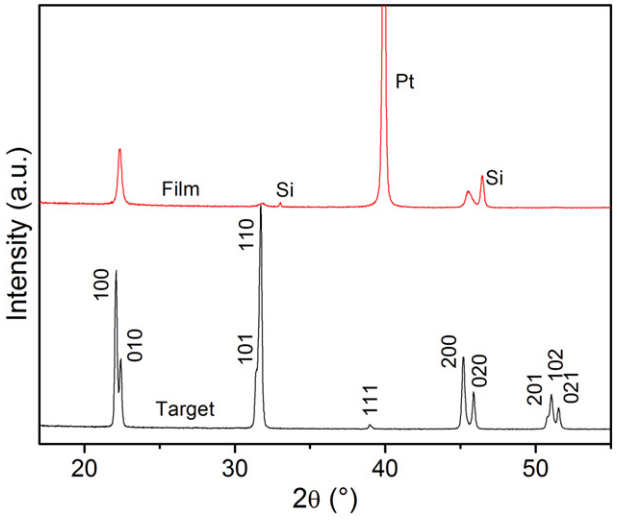

Fig. 1. XRD patterns of the ceramic target sintered at 1060 °C, and KNN5 film prepared at 800 °C, 10 Hz and 16 Pa of oxygen pressure.

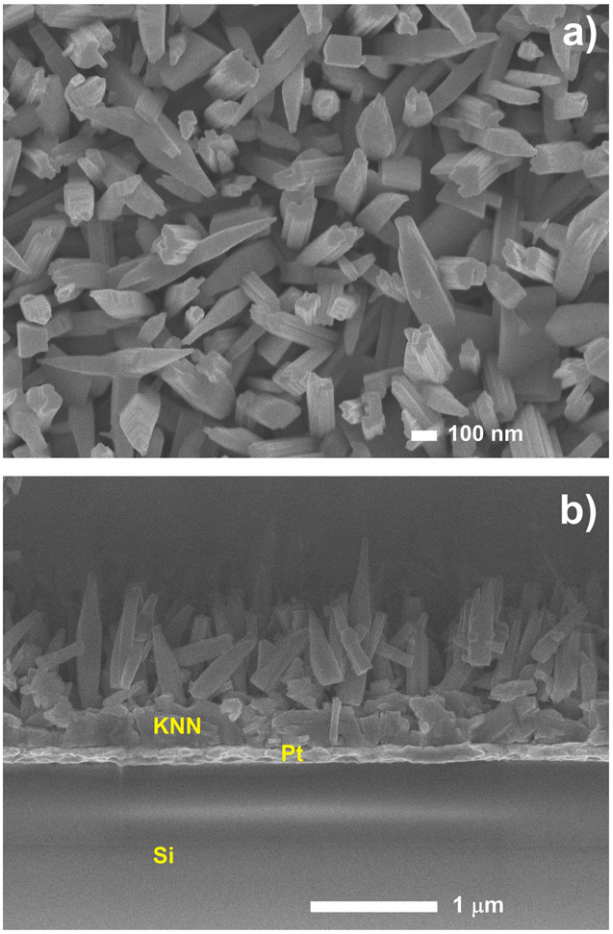

Fig. 2. (a) Top and (b) transversal SEM images of KNN5 thin films grown at 800 °C, 10 Hz and 16 Pa of oxygen pressure.

In order to promote densification and homogeneity in the films, the deposition parameters were changed. Reducing the deposition temperature, while maintaining all the other parameters constant, the thin films gradually transforms the columnar growth observed at 800 °C, into to a completely cubic-like morphology at 675 °C, with a wide grain size distribution characteristic of these compounds, as can be seen in Fig. 3. Moreover, the crystal average size for KNN2 and KNN3 (Fig. 3c and d) are 132 and 86 nm, respectively. This indicates that reducing the deposition temperature it was obtained smaller crystal and size distribution. Fig. 4 shows how the oxygen partial pressure affects the crystal phase of the films. For the lower pressure used (8 Pa KNN1 in Table 1), tungsten-bronze peaks of $K_6Nb_{10.8}O_{30}$ are observed, perhaps because the available oxygen is not enough to produce the perovskite structure. Increasing the oxygen pressure to 16 and 32 Pa generates the pure orthorhombic KNN. Other important SEM images of films prepared at different oxygen partial pressures are shown in Fig. 5. As can be seen, there is no a significant variation in crystal size and morphology, even for the sample with a prevalent tungsten-bronze phase, the one prepared at 8 Pa.

In agreement with the above analysis, although a pure KNN perovskite crystal structure is obtained using 16 and 32 Pa, these higher oxygen pressures may have a more important effect: avoiding oxygen vacancy formation and consequently, reducing dielectric losses. Furthermore, to prevent the columnar, loosely-packed morphology observed in films grown at high temperatures, i.e. at 800 °C, but at the same time ensuring pure KNN crystal phase formation, 725 °C was chosen as the optimal temperature and the laser frequency was lowered from 10 Hz to 5 Hz.

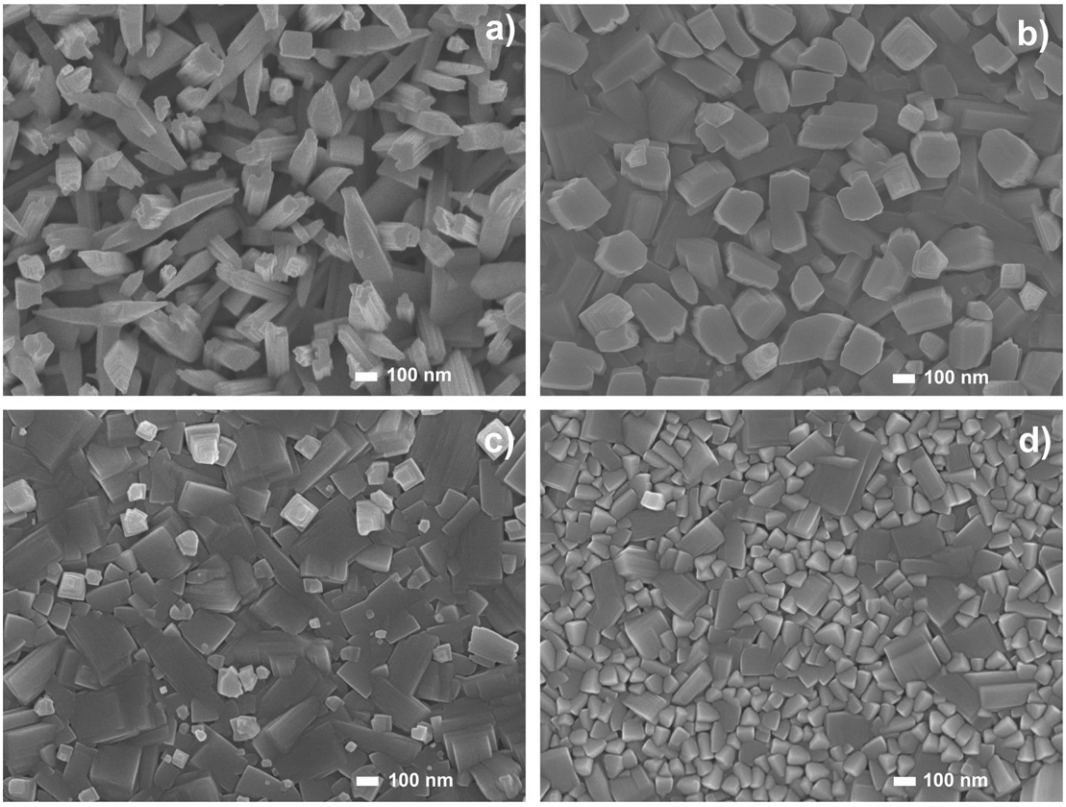

Fig. 3. SEM images of: (a) KNN5, (b) KNN4, (c) KNN2 and (d) KNN3 thin films grown at 16 Pa and 800, 750, 700 and 675 °C, respectively.

As a consequence, a more homogeneous and compact film was obtained, as is seen in the SEM images in Fig. 6. The quasi-cubic crystal shape observed in these images is typical of the orthorhombic KNN structure and similar compositions [19–20]. In this case, (100), (010) and (001) crystal facets are observed because of their lower energy formation [19].

In KNN thin films and ceramics, secondary phases appear due to the potassium and sodium losses, which create oxygen vacancies and increase the electrical conductivity [21]. This has impeded the determination of clear piezo-ferroelectric responses in KNN films with thicknesses as low as the ones studied in this work, of around 165 nm. In our case, pure KNN films were obtained as was shown in Fig. 4, and also, by using piezoresponse force microscopy (PFM), well-defined piezoelectric as well as ferroelectric responses were detected, as observed in Figs. 7 and 8. Fig. 7 shows the amplitude and phase PFM images of the film prepared at 725 °C and 32 Pa oxygen pressure. The well-defined dark and light contrast in the phase-PFM image (Fig. 7b) indicate ferroelectric domains with out of plane polarization components in opposite directions, while domain wall boundaries are associated with the dark contours observed in the amplitude-PFM image (Fig. 7a).

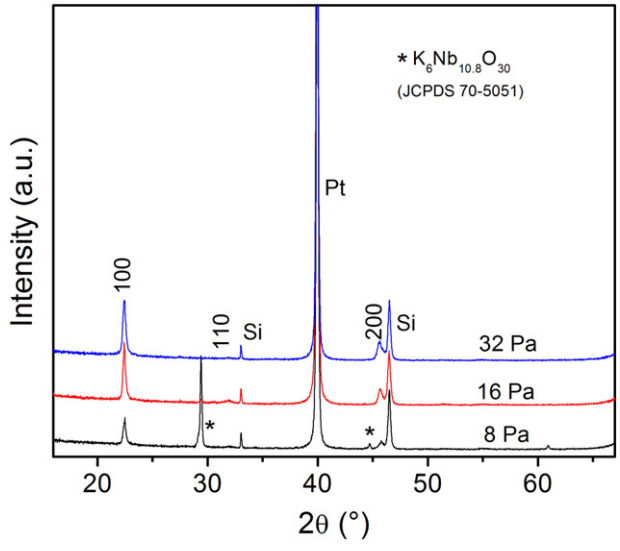

Fig. 4. XRD patterns of KNN1, KNN2 and KNN6 films grown at 700 °C and different oxygen pressures.

Polarization reversal was achieved by applying a *dc* bias of + 10 V in an 8 × 8 μm^2 area, and then − 10 V in a 4 × 4 μm^2 sub square inside the first zone. Again, the change in contrast from dark to light areas in the phase-PFM image in Fig. 8b is associated with opposite polarization directions, while the delimitation between regions with opposite polarization directions appear as dark lines on the amplitude-PFM image in Fig. 8a, this shows, ferroelectricity.

By using contact resonance-PFM [22] local amplitude and phase hysteresis curves, see Fig. 9, were measured. A coercive voltage of ~3.5 V was calculated from the well-defined ferroelectric hysteresis loop, while a d_{33} piezoelectric coefficient of 37 pm/V was calculated using the amplitude-PFM graph, which shows the typical butterfly shape expected for ferroelectric materials. These results are between those reported in KNN films prepared by sol-gel synthesis without excess alkaline elements [7]; by PLD using a Li^{+1}/Ta^{+5} doped KNN target [10] and by sputtering using different substrates [12].

Finally, the time signal and frequency responses are shown in Fig. 10 a) and b), respectively; these graphs summarize the principal features of a prototypic ultrasonic sensor for wave in thickness (build with the KNN-thin film, between platinum-gold electrodes over a Si-substrate, dimensions of the whole device were 1 × 1 cm^2, by 300 μm thickness). Essentially, the generation of ultrasound signals by absorbed laser pulses is the photoacoustic effect [23]. In fact, the acoustic signal contains a great deal of information on the interaction between the inner material structure and the pressure waves produced by the incident

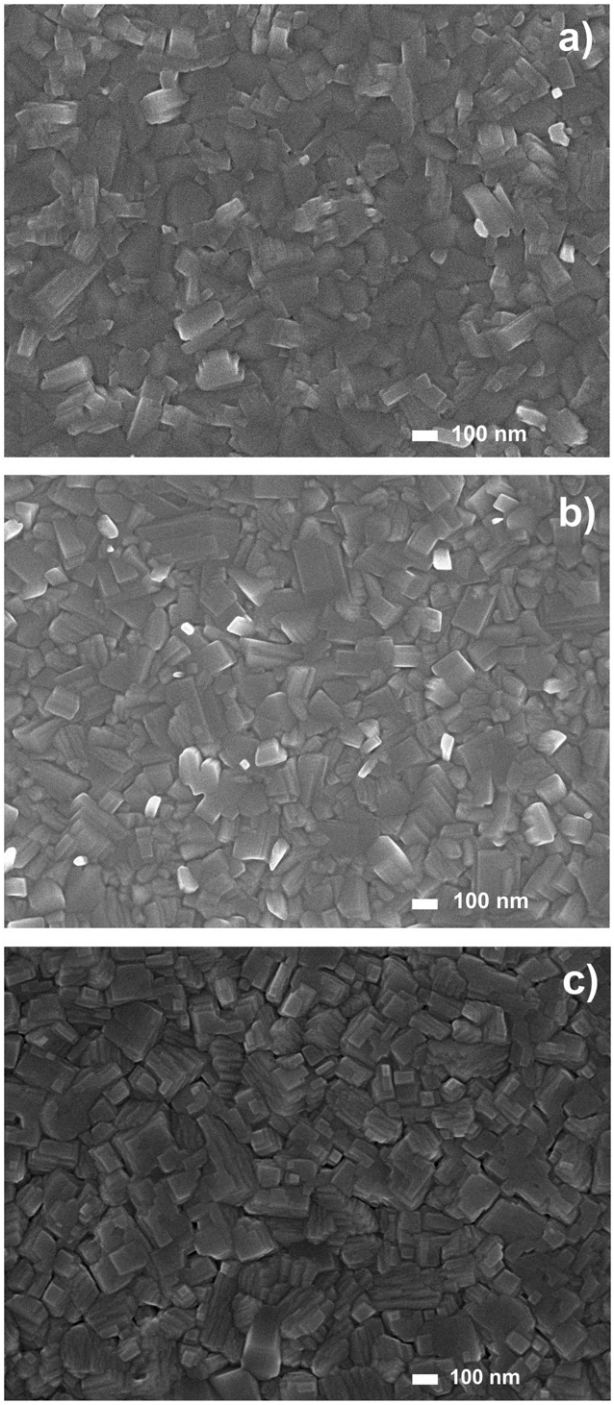

Fig. 5. SEM images of a) KNN1, b) KNN2 and c) KNN6 films grown at 700 °C and 8, 16 and 32 Pa oxygen pressures.

laser beam. For example, the ultrasonic waves activate different rates of stress and strain in the lattice, which change the local volume as a function of the pressure wave; i.e. the pressure wave causes the mechanical stressed states in the material. In particular, we implemented the photoacoustic technique using laser pulses —a Nd:YAG laser system (Continuum, model: Surelite I) @10 Hz, and pulse-width of 5 ns)— for excitation of the medium and a piezoelectric sensor for detection of the ultrasonic response. The absorption pulse leads to the generation of a broadband thermoelastic pressure wave (which propagates through the medium at its speed of sound, and reaches the piezoelectric sensor), for that reason it is common to obtain a complicated spectrum. This approach to the photoacoustic technique, using laser pulses for

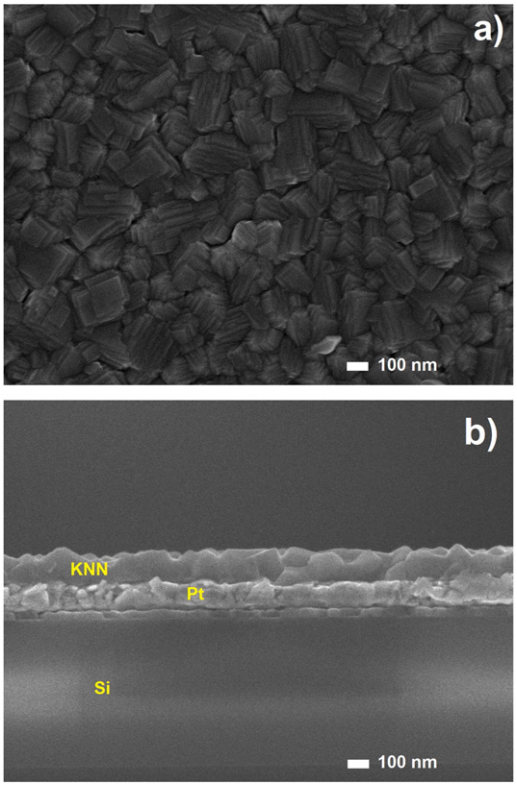

Fig. 6. (a) Top and (b) transversal SEM images of KNN7 film prepared at 725 °C, 5 Hz and 32 Pa.

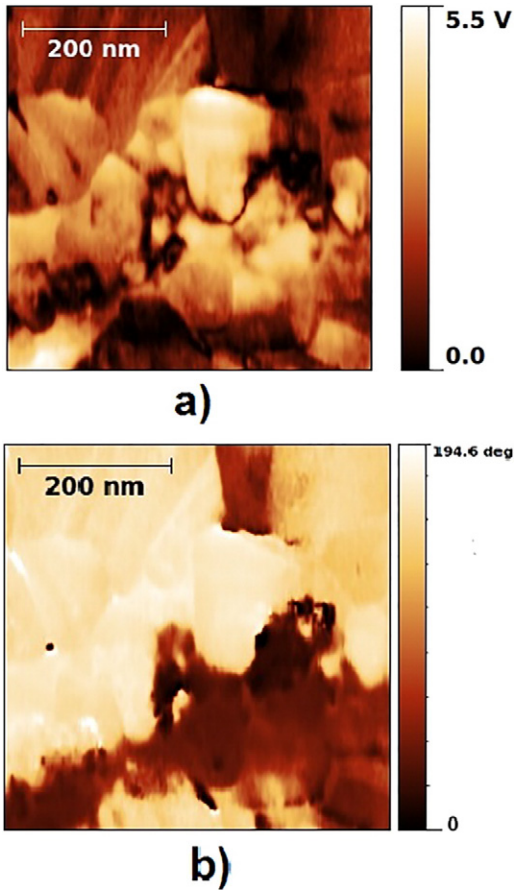

Fig. 7. (a) amplitude and (b) phase PFM images of KNN7 film prepared at 725 °C, 5 Hz and 32 Pa.

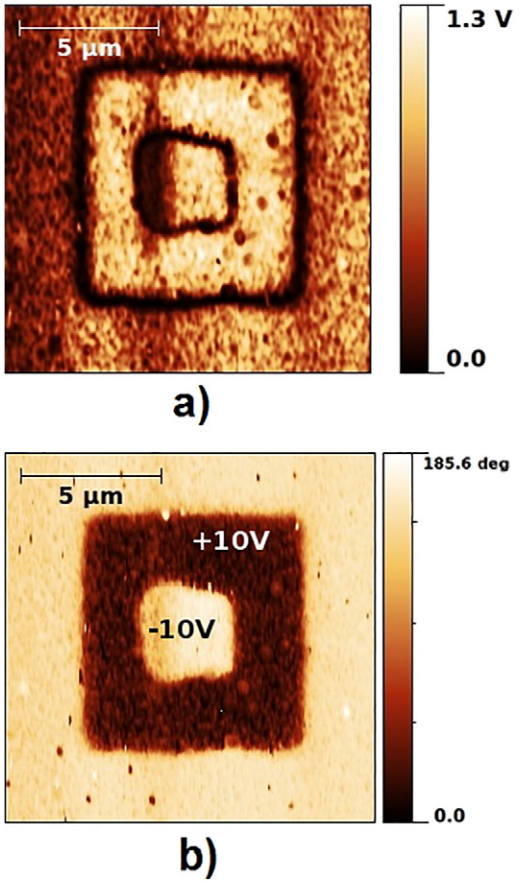

Fig. 8. (a) amplitude and (b) phase PFM images of KNN7 film prepared at 725 °C, 5 Hz and 32 Pa, after being poled with ±10 V.

excitation and piezoelectric detection, has been successfully used for the analysis of structural phase transitions [24–25]. In this case we use the same sensor to obtain the time-response on a 230 nm thick KNN thin film, and it was found that the resonant frequency was approximately of 3 MHz, but with a response up to 20 MHz. It is well known that transduction of any piezoelectric is maximum near the resonance frequency [26], so that the prepared thin film can be used as sensor close to 3 MHz where its performance is optimum.

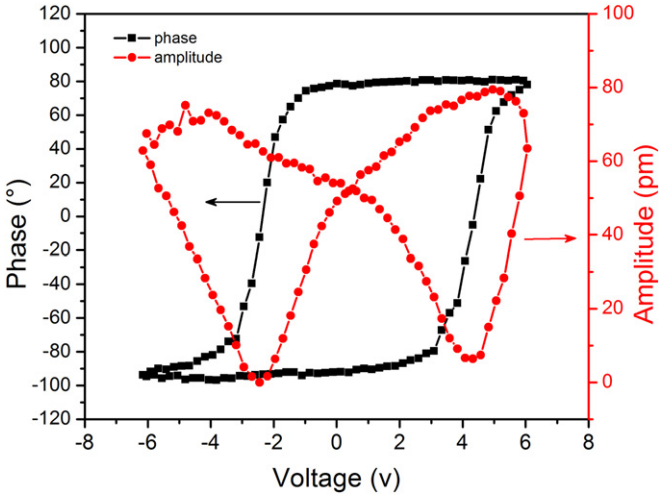

Fig. 9. Amplitude and phase-PFM curves of KNN7 film prepared at 725 °C, 5 Hz and 32 Pa.

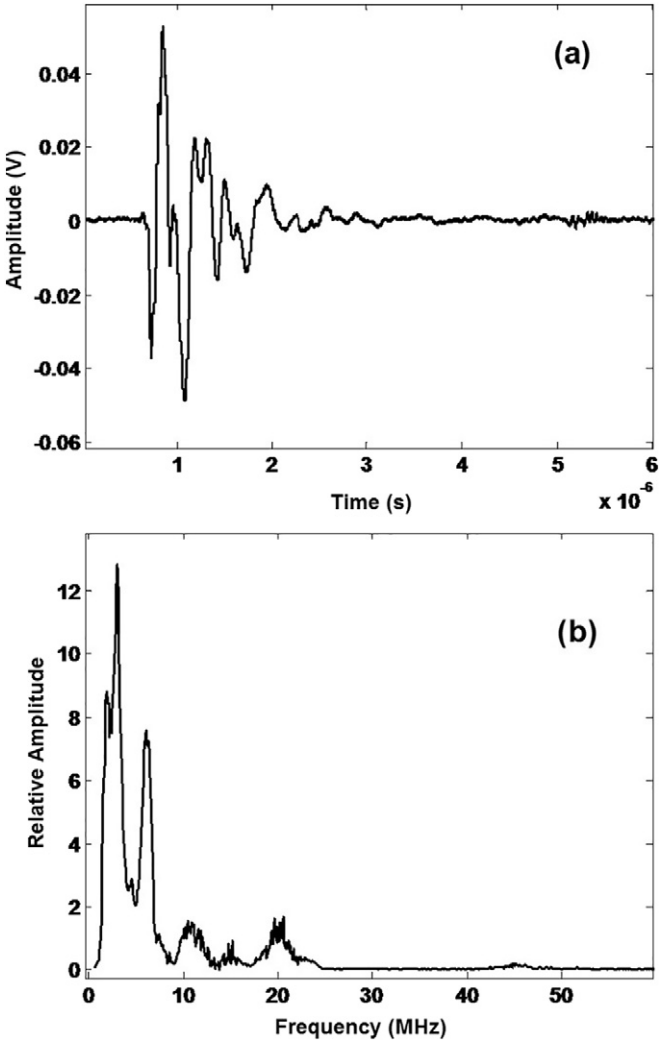

Fig. 10. Response of the thin film KNN device a) time signal, and b) frequency response.

4. Conclusions

Optimization of the oxygen pressure and temperature to 32 Pa and 725 °C, respectively in the PLD technique, gives rise to pure KNN perovskite structured films less than 200 nm thick, with an orthorhombic lattice, no secondary phases and a dense cubic-like morphology. The crystal structure remains if the oxygen pressure is reduced to 16 Pa, but for lower pressures, of 8 Pa, peaks of tungsten-bronze compound appear. Changing the deposition temperature from 670 to 800 °C does not affect the crystal structure, but a loosely packed columnar surface is produced if the temperature is as high as 800 °C. A clear ferroelectric response was achieved in KNN films as thin as 165 nm. From the well-defined phase and amplitude hysteresis curves, obtained by piezoresponse force microscopy, a coercive voltage of ~3.5 V and a d_{33} piezoelectric coefficient of 37 pm/V, were determined. Finally, we present a photoacoustic measurement of 230 nm thick KNN thin film, showing the sensor responds as a piezoelectric. It was found that the resonant frequency was approximately 3 MHz.

Acknowledgements

R. Castañeda-Guzmán kindly acknowledges PAPIIT-UNAM for support through project IG100314.

References

[1] G.H. Haertling, Ferroelectric ceramics: history and technology, J. Am. Ceram. Soc. 82 (1999) 797–818.
[2] Y. Saito, H. Takao, T. Tani, T. Nonoyama, K. Takatori, T. Homma, T. Nagaya, M. Nakamura, Lead-free piezoceramics, Nature 432 (2004) 84–87.
[3] Y. Shiratori, A. Magrez, C. Pithan, Particle size effect on the crystal structure symmetry of $K_{0.5}Na_{0.5}NbO_3$, J. Eur. Ceram. Soc. 25 (2005) 2075–2079.
[4] R. López, F. González, M.P. Cruz, M.E. Villafuerte-Castrejon, Piezoelectric and ferroelectric properties of $K_{0.5}Na_{0.5}NbO_3$ ceramics synthesized by spray drying method, Mater. Res. Bull. 46 (2011) 70–74.
[5] C.H. Wang, Physical and electric properties of lead-free $(Na_{0.5}K_{0.5})NbO_3$-$Ba(Zr_{0.04}Ti_{0.96})O_3$ ceramics, J. Ceram. Soc. Jpn. 117 (2009) 680–684.
[6] Y. Nakashima, W. Sakamoto, H. Maiwa, T. Shimura, T. Yogo, Lead-free piezoelectric $(K,Na)NbO_3$ thin films derived from metal alkoxide precursors, Jpn. J. Appl. Phys. 46 (2007) L311–L313.
[7] P.C. Goh, K. Yao, Z. Chen, Lead-free piezoelectric $_3)NbO_{0.5}Na_{0.5}$(K thin films derived from chemical solution modified with stabilizing agents, Appl. Phys. Lett. 97 (2010) 102901.
[8] G. Li, X.Q. Wu, W. Ren, P. Shi, X.F. Chen, X. Yao, Effects of excess amount of K and Na on properties of $(K_{0.48}Na_{0.52})NbO_3$ thin films, Ceram. Int. 38 (2012) S279–S281.
[9] L. Wang, W. Ren, K. Yao, P. Shi, X. Wu, X. Yao, Effects of thickness on structures and electrical properties of $K_{0.5}Na_{0.5}NbO_3$ thick films derived from polyvinylpyrrolidone-modified chemical solution, Ceram. Int. 38 (2012) S291–S294.
[10] D.Y. Wang, D.M. Lin, K.W. Kwok, N.Y. Chan, J.Y. Dai, S. Li, H.L.W. Chan, Ferroelectric, piezoelectric, and leakage current properties of $_3)O_{0.225}Ta_{0.775})(Nb_{0.04}Li_{0.48}Na_{0.48}$(K thin films grown by pulsed laser deposition, Appl. Phys. Lett. 98 (2011) 022902.
[11] M. Zhu, X. Shang, G. Chang, M. Li, X. Liu, T. Zhou, Y. He, Pulsed laser deposition of single-phase lead-free NKLNST thin films with K- and Na-excess targets, J. Alloys Compd. 567 (2013) 97–101.
[12] T. Li, G. Wang, K. Li, N. Sama, D. Remiens, X. Dong, Influence of LNO top electrodes on electrical properties of KNN/LNO thin films prepared by RF magnetron sputtering, J. Am. Ceram. Soc. 96 (2013) 787–790.
[13] I. Kanno, T. Ichida, K. Adachi, H. Kotera, K. Shibata, T. Mishima, Power-generation performance of lead-free $(K,Na)NbO_3$ piezoelectric thin-film energy harvesters, Sens. Actuators A 179 (2012) 132–136.
[14] K. Shibata, F. Oka, A. Ohishi, T. Mishima, I. Kanno, Piezoelectric properties of $(K,Na)NbO_3$ films deposited by rf magnetron sputtering, Appl. Phys. Express 1 (2008), 011501. .
[15] K. Wang, B.P. Zhang, J.F. Li, L.M. Zhang, Lead-free $Na_{0.5}K_{0.5}NbO_3$ piezoelectric ceramics fabricated by spark plasma sintering: annealing effect on electrical properties, J. Electroceram. 21 (2007) 251–254.
[16] J.A. Peña-Jiménez, F. González, R. López-Juárez, J.M. Hernández-Alcántara, E. Camarillo, H. Murrieta-Sánchez, L. Pardo, M.E. Villafuerte-Castrejón, Optical and piezoelectric study of KNN solid solutions co-doped with La-Mn and Eu-Fe, Materials 9 (2016) 805.
[17] L. Wang, W. Ren, P. Shi, X. Chen, X. Wu, X. Yao, Enhanced ferroelectric properties in Mn-doped $K_{0.5}Na_{0.5}NbO_3$ thin films derived from chemical solution deposition, Appl. Phys. Lett. 97 (2010) 072902.
[18] F. Lai, J.F. Li, Z.X. Zhu, Y. Xu, Influence of Li content on electrical properties of highly piezoelectric $(Li,K,Na)NbO_3$ thin films prepared by sol-gel processing, J. Appl. Phys. 106 (2009), 064101. .
[19] R. Lopez-Juarez, F. Gonzalez-Garcia, J. Zarate-Medina, R. Escalona-Gonzalez, S. Diaz de la Torre, M.E. Villafuerte-Castrejon, Piezoelectric properties of Li–Ta co-doped potassium–sodium niobate ceramics prepared by spark plasma and conventional sintering, J. Alloys Compd. 509 (2011) 3837–3842.
[20] J. Tellier, B. Malic, B. Dkhil, D. Jenko, J. Cilensek, M. Kosec, Crystal structure and phase transitions of sodium potassium niobate perovskites, Solid State Sci. 11 (2009) 320–324.
[21] H. Bruncková, Ľ. Medvecký, P. Hvizdoš, Effect of substrate on microstructure and mechanical properties of sol–gel prepared $(K,Na)NbO_3$ thin films, Mater. Sci. Eng. B 178 (2013) 254–262.
[22] E. Soergel, Piezoresponse force microscopy (PFM), J. Phys. D. Appl. Phys. 44 (2011) 464003.
[23] A.G. Bell, On the production and reproduction of sound by light, Am. J. Sci. 20 (1880) 305324.
[24] R. Castañeda Guzmán, M. Villagrán Muñiz, J.M. Saniger Blesa, O. Pérez-Martínez, Photoacoustic phase transition of the ceramic $_3$BaTiO, Appl. Phys. Lett. 73 (1998) 623.
[25] A. Huanosta-Tera, R. Castañeda-Guzmán, J.L. Pineda-Flores, Characterization of $Bi_{4-x}RxTi_3O_{12}$ (Rx = Pr, Nd, Gd, Dy, $x = 0.8$) layered electroceramics by a photoacoustic method, Mater. Res. Bull. 38 (2003) 1073–1079.
[26] B. Ren, S.W. Or, X. Zhao, H. Luo, Energy harvesting using a modified rectangular cymbal transducer based on $0.71Pb(Mg_{1/3}Nb_{2/3})O_3$–$0.29PbTiO_3$ single crystal, J. Appl. Phys. 107 (2010) 034501.